



Downregulation of lung mitochondrial prohibitin in COPD

Nikolaos Soultzis^a, Eirini Neofytou^a, Maria Psarrou^a,
Aristotelis Anagnostis^a, Nektarios Tavernarakis^b, Nikolaos Siafakas^a,
Eleni G. Tzortzaki^{a,*}

^a *Laboratory of Molecular and Cellular Pulmonology, Medical School, University of Crete, Heraklion, Greece*

^b *Institute of Molecular Biology and Biotechnology, Foundation for Research and Technology, Heraklion, Crete, Greece*

Received 3 January 2012; accepted 23 March 2012

Available online 20 April 2012

KEYWORDS

PHB1;
FEV₁;
Oxidative stress;
Reactive oxygen
species;
Smoking

Summary

Prohibitins (PHB1 and PHB2) are versatile proteins located at the inner mitochondrial membrane, maintaining normal mitochondrial function and morphology. They interact with the NADH dehydrogenase protein complex, which is essential for oxidoreductase activity within cells. However, their expression in lung epithelium, especially in smokers and patients with inflammatory lung diseases associated with increased oxidative stress, such as COPD, is unknown. Lung tissue specimens from 45 male subjects were studied: 20 COPD patients [age: 65.7 ± 5.8 years, smoking: 84.6 ± 33.6 pack-years, FEV₁ (%pred.): 58.7 ± 14.6 , FEV₁/FVC (%): 63.8 ± 9.4], 15 non-COPD smokers [age: 59.0 ± 12.1 years, smoking: 52.5 ± 20.8 pack-years, FEV₁ (%pred.): 85.5 ± 14.2 , FEV₁/FVC (%): 78.5 ± 4.7] and 10 non-smokers. Quantitative real-time PCR experiments were carried out for PHB1 and PHB2, using β -actin as internal control. Non-COPD smokers exhibited lower PHB1 mRNA levels when compared to non-smokers (0.55 ± 0.06 vs. 0.90 ± 0.06 , $P = 0.043$), while PHB1 expression was even further decreased in COPD patients (0.32 ± 0.02), a statistically significant finding vs. both non-COPD smokers ($P = 0.040$) and non-smokers ($P < 0.001$). By contrast, PHB2 levels were similar among the three study groups. Western blot analysis for the PHB1 protein verified the qPCR results (non-smokers: 1.77 ± 0.13 ; non-COPD smokers: 0.97 ± 0.08 ; COPD patients: 0.59 ± 0.10 , $P = 0.007$). Further analysis revealed that PHB1 downregulation in COPD patients cannot be attributed solely to smoking, and that PHB1 expression levels are associated with the degree of airway obstruction [FEV₁ ($P_{\text{mRNA}} = 0.004$, $P_{\text{protein}} = 0.014$)]. The significant downregulation of PHB1 in COPD and non-COPD smokers in comparison to non-smokers possibly reflects a distorted mitochondrial function due to decreased mitochondrial stability, especially in the mitochondria of COPD patients.

© 2012 Elsevier Ltd. All rights reserved.

* Corresponding author. Department of Thoracic Medicine, University Hospital of Heraklion, Medical School, University of Crete, 71110 Heraklion, Crete, Greece. Tel.: +30 2810 392433; fax: +30 2810 542650.

E-mail address: tzortzaki@med.uoc.gr (E.G. Tzortzaki).

Introduction

Chronic Obstructive Pulmonary Disease (COPD) is a multi-factorial cigarette smoking related disorder. Its clinical manifestations include chronic bronchitis, pulmonary emphysema and small airway disease, all of which eventually lead to the progressive destruction of lung parenchyma and to deterioration of lung function. Several mechanisms contribute to the pathogenesis of COPD, including influx of inflammatory cells into the lung, abnormal cellular growth, increased apoptotic events, extracellular matrix destruction and oxidative stress. Genetic background and infectious agents also play an important role.^{1–3}

External triggers such as tobacco smoke, noxious gases and viruses initiate local inflammation in the lung, enhancing oxidative stress. Reactive oxygen species (ROS) cause functional and structural alterations affecting redox-sensitive cellular processes such as mitochondrial function.⁴

The formation of oxidants, which are also produced within cells as by-products of normal metabolism, is balanced by antioxidants, which delay or hinder the oxidation process. A diverse group of molecules exhibit antioxidant properties; ranging from small molecules such as glutathione and vitamins C and E, to iron-binding protein chains, to enzymatic systems such as catalases, peroxidases and superoxide dismutases (SOD).⁵ These enzymes have isoforms with specific distribution: extracellular, cytosolic and particularly mitochondrial.^{6,7} Indeed, the majority of ROS compounds are formed during oxidative phosphorylation at the mitochondrial electron transport chain.⁸

The eukaryotic mitochondrial prohibitin (PHB) family comprises two members with ~53% amino acid homology, named prohibitin-1 (PHB1), a 30 kDa protein located at 17q21 and prohibitin 2 (PHB2 or REA), a 32 kDa protein located at 12p13.⁹ Both are ubiquitously expressed in eukaryotic cells, playing a significant role in several intracellular processes such as transcription regulation, apoptosis, cell cycle progression and aging,^{10–12} as well as in many diseases like obesity, diabetes and cancer.¹³ Prohibitins have been found in several cellular compartments, such as the plasma membrane and the nucleus,^{14,15} but are predominately localized in the inner mitochondrial membrane.¹⁶ PHB1 and PHB2 form heterodimers, which are the building blocks of large ring-shaped prohibitin complexes, with diameter of ~20–25 nm and >1 MDa

molecular mass.¹⁷ These complexes are essential components of the mitochondrial fusion machinery, maintaining mitochondrial stability, morphogenesis and normal function.^{18–20}

Recent findings suggest that prohibitin plays an important role in combating oxidative stress,¹³ by interacting with the NADH dehydrogenase subunits of the mitochondrial respiratory complex I, acting as complex I assembly chaperons.²¹ This has been observed in intestinal epithelial cells,²² in endothelial cells,²⁰ and in ex vivo rabbit lung experiments.²³ However, little is known about prohibitin expression and function in human lung tissue.

To gain insight into the involvement of prohibitin in redox changes associated with lung pathology, we determined the mRNA and protein levels of PHB1 and PHB2 in the lung epithelium, particularly under high ROS-generating conditions such as smoking, and in patients with inflammatory lung diseases associated with increased oxidative stress such as COPD, and we associated their expression with patients' anthropometric and spirometric values.

Materials and methods

Study subjects

The study was performed on lung tissue specimens from 45 male subjects who underwent open lung surgery for the excision of malignant solitary pulmonary nodule. Subjects were divided in three groups: a) 20 COPD current smokers, according to GOLD criteria,²⁴ b) 15 non-COPD current smokers and c) 10 non-smokers.

Smokers were defined as subjects who had a history of at least 20 pack-years of cigarette smoking. All subjects underwent routine pulmonary function testing. The GOLD spirometric classification of COPD severity, based on post-bronchodilator FEV₁ was used for the diagnosis of COPD. All COPD patients that participated in this study were GOLD stage II (FEV₁/FVC < 0.70, with 50% ≤ FEV₁ < 80% predicted) (Table 1).

The study was approved by the Medical Research Ethics Committee of the University Hospital of Heraklion and informed consent was obtained from all participants.

Tissue preparation

Human lung tissue samples were collected from all subjects from an uninvolved segment of the subpleural parenchyma

Table 1 Anthropometric characteristics and spirometric values of COPD patients, non-COPD smokers and non-smokers.

	COPD patients (n = 20)	Non-COPD smokers (n = 15)	Non-smokers (n = 10)	P-value ^a
Age (years)	65.7 ± 5.8	59.0 ± 12.1	58.5 ± 12.1	0.065
Smoking (P-Y)	84.6 ± 33.6	52.5 ± 20.8	–	0.002
FEV ₁ (% pred.)	58.7 ± 14.6	85.5 ± 14.2	105.3 ± 8.5	<0.001
FVC (% pred.)	73.4 ± 15.3	86.1 ± 12.7	112.0 ± 14.0	0.006
FEV ₁ /FVC (%)	63.8 ± 9.4	78.5 ± 4.7	79.3 ± 3.2	<0.001

P-Y: pack-years of smoking (mean ± SD).

FEV₁: forced expiratory volume in 1st second (mean ± SD).

FVC: forced vital capacity (mean ± SD).

^a Kruskal–Wallis H test.

at least 5 cm away from the solitary nodule. Samples were immediately frozen in liquid nitrogen and stored at -80°C until use.

RNA extraction and cDNA preparation

Lung tissue specimens (~ 100 mg) were homogenized in TRIzol[®] reagent (Invitrogen, Carlsbad, CA) using a power homogenizer and incubated at room temperature, followed by the addition of chloroform and centrifugation. Total RNA was precipitated from the supernatant with isopropanol, washed with 75% ethanol and resuspended in 20 μl of DEPC-treated water. RNA concentration and purity were calculated after measuring on a NanoDrop 1000 spectrophotometer (NanoDrop Products, Wilmington, DE) its 260 nm absorbance and 260/280 nm and 260/230 nm absorbance ratios, respectively. Representative samples were also run on agarose gels, in order to verify that RNA was not fragmented.

cDNA was synthesized by reverse transcription (RT) with the RETROscript[®] Kit (Ambion, Austin, TX), using random decamers as amplification primers. In detail, 2.5 μg of total RNA and 5 μM of random decamers were heated at 80°C for 3 min, in order to remove RNA secondary structures, and placed on ice until the addition of cDNA synthesis mix, which contained 1 \times RT Buffer, 0.5 mM dNTPs Mix, 10 units RNase Inhibitor and 100 units MMLV-RT reverse transcriptase. The final mix (volume 20 μl) was incubated at 55°C for 1 h. The reaction was terminated by heating at 92°C for 10 min and cDNA was stored at -20°C until use.

Quantitative real-time polymerase chain reaction assay

PHB1 and PHB2 mRNA expression was measured using a real-time qPCR assay with the SYBR[®] Green I dye. A housekeeping gene, beta-actin (β -actin), was used as an internal control, in order to normalize PHB1 and PHB2 mRNA expression levels. The mRNA-specific primers, which were designed with the Lasergene[®] 7.0 software (DNASTAR, Madison, WI) and span at least one intron with an average length >800 bp, are listed in Table 2. After initial experiments, in order to optimize the concentration and annealing temperature of the primers, cDNA from all study subjects (1 μl) was amplified in a PCR reaction containing 2 \times Maxima[™] SYBR Green qPCR Master Mix (Fermentas, Glen Burnie, MD) (containing 2.5 mM MgCl_2) and 300 nM of each

primer in a final volume of 20 μl . To ensure the accuracy of the quantification measurements, a representative pool of all samples was diluted in a series of six 2 \times dilutions and was run on the same plate, in order to construct a standard curve for the quantification process. After initial denaturation at 95°C for 10 min, samples were subjected to 40 cycles of amplification, comprised of denaturation at 95°C for 20 s, annealing at 60°C (β -actin) or 58°C (PHB1 and PHB2) for 30 s and elongation at 72°C for 30 s, followed by a melt curve analysis, in which the temperature was increased from 60°C to 95°C at a linear rate of 0.2 $^{\circ}\text{C}/\text{s}$. Data collection was performed during both annealing and extension, with two measurements at each step, and at all times during the melt curve analysis. PCR experiments were conducted on an Mx3000P real-time PCR thermal cycler using software version 4.10, Build 389 Schema 85 (Stratagene, La Jolla, CA). Verification of the PCR products, in terms of correct size and the absence of dimers, was conducted using a 2% (w/v) agarose gel electrophoresis. After amplification, standard curves were constructed from the samples used in the series of consecutive dilutions. Subsequently, using these standard curves and the Ct value of the samples, we calculated the mRNA expression of the genes studied (Fig. 1). Samples with no amplification plots or with dissociation curves that exhibited signs of primer-dimer formation or by-products were excluded. To normalize the mRNA expression of each gene, its value was divided by the same sample's β -actin mRNA value. In each PCR reaction two negative controls were included, one with no cDNA template and one with no reverse transcription treatment. All qPCR measurements were conducted in triplicates.

Protein extraction

Lung tissue samples (~ 100 mg) were dissolved in 2 ml of T-PER[®] Tissue Protein Extraction Reagent (Thermo Fisher Scientific, Waltham, MA) with added HALT[™] Protease and Phosphatase Inhibitor Cocktails (Thermo Scientific) and homogenized. After centrifugation at 10,000 g for 5 min (Fig. 1) to pellet tissue debris, the supernatant was collected and stored at -80°C until use.

Western blot

Western blot detection of PHB1 (30 kDa) and β -actin (43 kDa), which was used as internal control, was performed using standard protocols. Sample preparations of each lung protein specimen (30 μg) were separated by 12.5% SDS-polyacrylamide gel electrophoresis, using β -mercaptoethanol as reducing agent. The proteins were then transferred electrophoretically from the gels to a 0.45 μm nitrocellulose membrane (Thermo Scientific). Membranes were incubated with 1 $\mu\text{g}/\text{ml}$ of mouse anti-PHB1 monoclonal antibody MS-261-P1ABX (Thermo Scientific). After applying the AP124P goat anti-mouse peroxidase conjugated secondary antibody (Millipore, Billerica, MA), immunodetection was performed with the SuperSignal[®] West Pico Chemiluminescent Substrate (Thermo Scientific), detected on Super RX X-ray films (Fujifilm, Japan). The mouse anti-actin antibody MAB1501 (Millipore) was used in order to normalize PHB1 protein expression.

Table 2 Primer sequences used for quantitative real-time PCR.

Primer pair	Sequence (5'–3')	Amplicon size (bp)
PHB1	GCG TGG TGA ACT CTG CCT TA TGT ACC CAC GGG ATG AGA AA	124
PHB2	CCG AGG GCC TTC ACT TCA CCT GTA GGG GAG GAG ATT TTT C	91
β -actin	CGG CAT CGT CAC CAA CTG GGC ACA CGC AGC TCA TTG	70

Films were scanned and protein lanes were quantified using the Photoshop CS2 image analysis software (Adobe Systems, San Jose, CA) (Fig. 1).

Statistical analysis

Prohibitin mRNA and protein levels were first evaluated by the one-sample Kolmogorov–Smirnov goodness-of-fit test, in order to determine whether they follow a normal distribution pattern. Depending on the results, Pearson's or the non-parametric Spearman's rank correlation was used to examine their association with continuous variables (age, pack-years, spirometric values). Moreover, their association with categorical data (smoking status) was examined using Student's *t*-test (after examining for equality of variances with Levene's test), or its non-parametric equivalents Mann–Whitney U and Kruskal–Wallis H tests. Additionally, the Chi-square (χ^2) test, replaced by Fisher's exact test when indicated by the analysis, was used to examine PHB1 and PHB2 expression status with the various clinicopathological parameters after stratification. Finally, univariate analysis was used to correct crude *p*-values (P_c) for age and pack-years of smoking, producing adjusted *p*-values (P_a). Statistical analyses were 2-sided and performed with SPSS 11.5 (SPSS, Chicago, IL). Statistical significance was set at the 95% level ($P < 0.05$).

Results

Clinical characteristics of the study groups

The anthropometric characteristics and spirometric values of the three study groups (non-smokers, non-COPD smokers and COPD smokers) are shown in Table 1. As expected from the selection criteria, smokers with COPD had a significantly lower value of FEV₁, FVC and FEV₁/FVC ratio than

non-COPD smokers ($P_{FEV_1} = 0.001$, $P_{FVC} = 0.039$, $P_{FEV_1/FVC} < 0.001$, respectively). In contrast, smoking exposure was higher in COPD patients versus non-COPD smokers (84.6 ± 33.6 pack-years vs. 52.5 ± 20.8 pack-years, $P = 0.012$). Finally, although non-COPD smokers were on average ~ 7 years younger than COPD smokers, this age difference was not statistically significant ($P = 0.11$) Table 1.

Quantitative real-time PCR analysis

Non-COPD smokers exhibited lower PHB1 mRNA levels when compared to non-smokers (0.55 ± 0.06 vs. 0.90 ± 0.06 , $P_c = 0.011$, $P_a = 0.043$), while PHB1 expression was even further decreased in COPD patients (0.32 ± 0.02), a finding statistically significant vs. both non-COPD smokers ($P_c = 0.012$, $P_a = 0.040$) and non-smokers ($P_c = 0.009$, $P_a < 0.001$) (Fig. 2). In contrast, PHB2 levels were similar among the three study groups (non-smokers: 0.97 ± 0.12 ; non-COPD smokers: 1.01 ± 0.08 ; COPD patients: 0.95 ± 0.13 ; $P_c = 0.85$, $P_a = 0.69$) (Fig. 2).

Western blot analysis

Western blot analysis of PHB1 verified the above results, since PHB1 protein levels also decreased from non-smokers to non-COPD smokers to COPD patients, and with a similar decrease rate as mRNA levels (non-smokers: 1.77 ± 0.13 ; non-COPD smokers: 0.97 ± 0.08 ; COPD patients: 0.59 ± 0.10 , $P_c = 0.026$, $P_a = 0.007$) (Fig. 2).

PHB1 expression was not associated with the amount of smoking exposure in COPD patients

In order to determine whether the decrease in PHB1 levels among COPD patients was only attributed to smoking, we

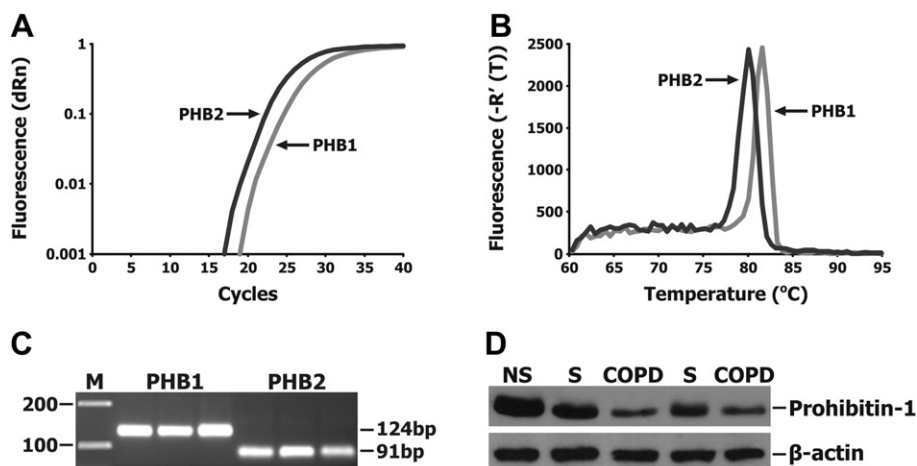


Figure 1 Representative examples of quantitative real-time PCR using SYBR[®] Green I detection dye: (A) Amplification plots and (B) Dissociation curves of PHB1 and PHB2; (C) Representative examples of PCR products from the two prohibitin family members after electrophoresis in a 2% (w/v) agarose gel and staining with ethidium bromide. M: 100-bp DNA ladder; (D) Representative examples of prohibitin-1 Western blot analysis in non-smokers (NS), non-COPD smokers (S) and COPD patients (COPD). β -actin was used as internal control.

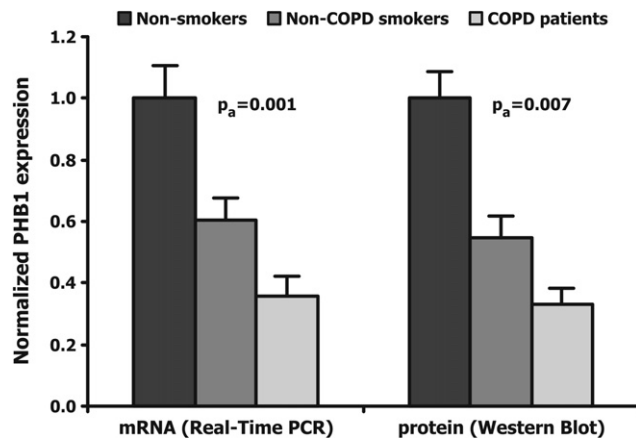


Figure 2 mRNA and protein expression of PHB1 in the three study groups (non-smokers, non-COPD smokers, COPD patients). Expression levels are normalized based on the non-smokers group. Error bars represent each category's SEM (standard error of the mean). P_a : adjusted p -values corrected for age and pack-year of smoking.

divided our COPD patients to 2 sub-groups, one with high pack-years (>100) and one with smoking exposure comparable to non-COPD smokers (Table 3). Both PHB1 mRNA and protein levels were approximately even between the two COPD sub-groups (mRNA: 0.31 ± 0.02 vs. 0.34 ± 0.02 , $P_c = 0.40$, $P_a = 0.84$; protein: 0.58 ± 0.14 vs. 0.59 ± 0.15 , $P_c = 0.97$, $P_a = 0.54$) and ~40% decreased from PHB1 levels in non-COPD smokers (mRNA: 0.55 ± 0.06 ; protein: 0.97 ± 0.08) (Fig. 3).

PHB1 expression is associated with the severity of airflow obstruction (FEV_1)

Scatter plot analysis of PHB1 expression in relation to FEV_1 showed that COPD patients and non-COPD smokers form distinct clusters, resulting in a positive association of PHB1 expression levels with FEV_1 ($P_{mRNA} = 0.004$ and $P_{protein} = 0.014$) (Fig. 4). In contrast, no statistically

significant association was observed between PHB1 mRNA or protein levels with patients' age or years of smoking exposure.

Discussion

In the present study, we investigated the expression of the two human prohibitin family members, PHB1 and PHB2, in COPD patients, non-COPD smokers and non-smokers. Given the critical role of the prohibitin complex in mitochondrial biogenesis and function, we aimed to evaluate the potential implication of mitochondrial integrity maintenance mechanisms in lung epithelium damage. We were able to demonstrate that PHB1 mRNA and protein levels decrease at a linear rate from non-smokers to non-COPD smokers to COPD patients, while PHB2 expression remained steady among the three study groups. We also established that, for COPD patients, this decrease was not related to age or smoking intensity, but rather to the degree of airway obstruction (FEV_1). To our knowledge, this is the first study reporting on prohibitin expression levels in the human lung epithelium.

The model we propose for the gradual PHB1 downregulation is the following: Smoking increases production of ROS that damages the mitochondrial respiratory machinery, leading to cellular damage and the downregulation of PHB1. In COPD, since there is an increased inflammatory response, the production of ROS is further elevated, damaging lung epithelial cells, impairing mitochondrial integrity, and thus decreasing PHB1 expression to even lower levels.

Prohibitin mitochondrial complexes are important for the stability of the inner mitochondrial membrane, which is essential for maintaining intracellular respiratory functions. Prohibitin also acts as a chaperone of the mitochondrial complex I, and especially of the NADH dehydrogenase subunits, which are important for the NADH:ubiquinone oxidoreductase activity, a key enzymatic activity for detoxification and metabolizing toxins and other dangerous substances inhaled by smoking.²⁵ When PHB1 is downregulated, the large PHB1/PHB2 ring-shaped transmembrane complexes cannot form, resulting in the

Table 3 Anthropometric characteristics and spirometric values of COPD patients after categorization into two groups according to smoking exposure (heavy and light smokers), versus non-COPD smokers.

	COPD patients		Non-COPD smokers ($n = 15$)	P -value ^c	
	Heavy smokers ($n = 11$)	Light smokers ($n = 9$)			
Age (years)	65.0 ± 6.1	66.5 ± 5.8	59.0 ± 12.1	0.20 ^a	0.17 ^b
Smoking (P-Y)	112.1 ± 10.7	52.5 ± 16.4	52.5 ± 20.8	0.001 ^a	0.54 ^b
FEV_1 (% pred.)	62.4 ± 17.8	54.4 ± 9.6	85.5 ± 14.2	0.013 ^a	0.003 ^b
FVC (% pred.)	75.4 ± 17.7	71.1 ± 13.3	86.1 ± 12.7	0.16 ^a	0.044 ^b
FEV_1/FVC (%)	63.0 ± 9.2	64.9 ± 10.4	78.5 ± 4.7	0.001 ^a	0.001 ^b

P-Y: pack-years of smoking (mean \pm SD).

FEV_1 : forced expiratory volume in 1st second (mean \pm SD).

FVC: forced vital capacity (mean \pm SD).

^a COPD heavy smokers vs. non-COPD smokers.

^b COPD light smokers vs. non-COPD smokers.

^c Mann-Whitney U test.

loss of NADH reductase activity, which in turn increases the levels of ROS within cells, eventually leading to their death.

PHB1 downregulation among COPD patients cannot be attributed to smoking alone, since COPD patients with pack-years comparable to non-COPD smokers (~52py) and COPD patients with more than 100py had approximately the same prohibitin-1 expression. If PHB1 expression was correlated with the amount of smoking exposure, then COPD patients with high tobacco consumption would have lower prohibitin-1 mRNA and protein levels than those observed. Therefore, there are other factors that contribute to this effect. Possibly, the inflammatory response, greatly increased in COPD patients,⁴ leads to increased ROS production and faster cellular damage than in smokers, which could explain the difference in PHB1 expression between COPD patients and non-COPD smokers.

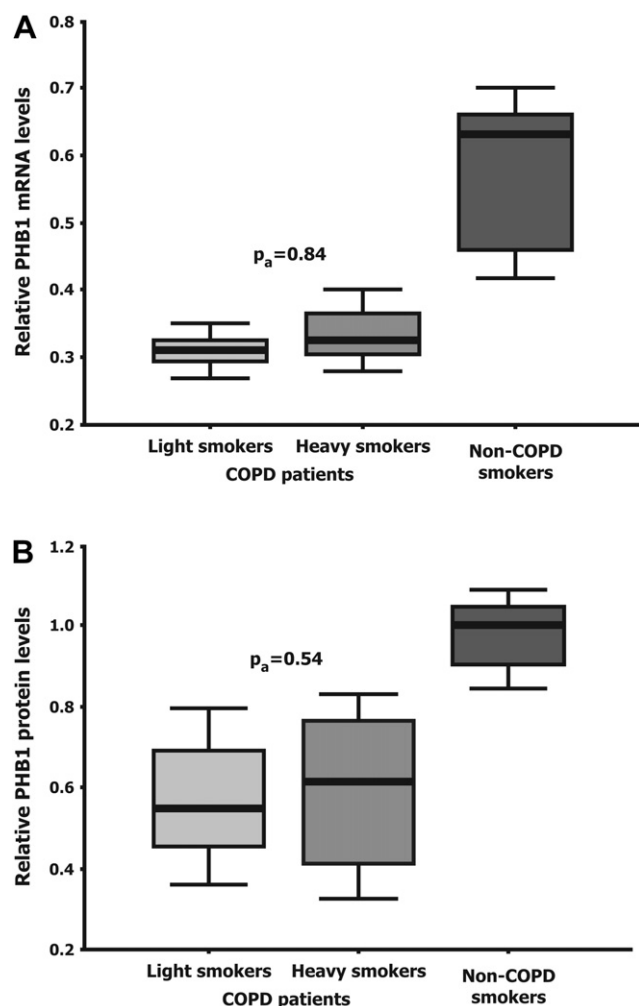


Figure 3 Box and whisker plots depicting relative (A) mRNA and (B) Protein expression of PHB1, according to smoking exposure (COPD patients with high pack-years, COPD patients with low pack-years, non-COPD smokers). The thick line near the center of each rectangular box represents the median value, the bottom and top edges of the box indicate the 1st (Q_1) and 3rd (Q_3) quartiles, and the ends of the whiskers depict the 10th (P_{10}) and 90th (P_{90}) percentiles. P_a : adjusted p -values corrected for age and pack-year of smoking.

The finding that only PHB1 was downregulated in non-COPD smokers and COPD patients and not PHB2, is not unexpected. Knock-out studies in cells have shown that when either PHB1 or PHB2 is not expressed then their ring-shaped complex is not formed.²⁶ Therefore, loss of only one prohibitin protein is sufficient for the disruption of the mitochondrial respiratory machinery.

Age is also considered a risk factor for COPD, not only due to the steady accumulation of free radicals, heavy metals and other by-products of the metabolism within cells, which leads to their death, but also because with age there is a progressive air space enlargement in the lungs, which decreases airflow.²⁷ However, since PHB1 expression was not statistically associated with age, the small age difference among our study groups cannot account for the observed PHB1 expression differences. Univariate analysis verified that, since all statistically confirmed associations retained their significance even after correction with age and pack-years of smoking.

In a previous study conducted by our group on the same samples pool, it was demonstrated that in COPD patients there is a shift in balance in favor of pro-apoptotic molecule p53 instead of the anti-apoptotic molecule bcl-2.²⁸ PHB1 downregulation leads to increased ROS formation and oxidative DNA damage, which directs cells to apoptosis, explaining the increased p53 levels we observed.

Although smoking did not have a dose-dependent effect on PHB1 expression, FEV₁ was associated with low PHB1 levels. This reflects a deteriorating mitochondrial stability as COPD progresses.

According to the GOLD guidelines, our COPD patients were categorized as GOLD stage II. It would be interesting to expand the study to include patients from the other three COPD categories (GOLD stages I, III and IV), in order to investigate the expression levels of prohibitin in those groups, and to determine if and why there are any differences in the expression of PHB1 among the four COPD categories.

One thing that should be taken into consideration is the fact that tissue samples were taken from patients that underwent lung surgery for malignant solitary nodule removal. However, our data have not been compromised by the inclusion of cancer cells in the analysis, since the tissue samples that were obtained for our study were not close to the malignant region.

A limitation of our study could be that biopsy specimens likely compromise multiple cell types. Histological evaluations conducted in previous studies by our group in the same sample types (COPD patients and non-COPD smokers) suggest that the most dominant cell type within the lung epithelium of smokers and COPD patients is type II pneumocytes, along with a substantial number of alveolar macrophages.^{28,29} Whether our results reflect mitochondrial changes within pneumocytes or macrophages cannot be determined without performing tissue laser microdissection.

In conclusion, our study revealed decreased PHB1 levels in non-COPD smokers and especially in COPD patients, reflecting a reduced mitochondrial stability that possibly results in decreased antioxidant capacity, especially in the mitochondria of COPD patients. Further studies are needed to verify and expand the findings reported here.

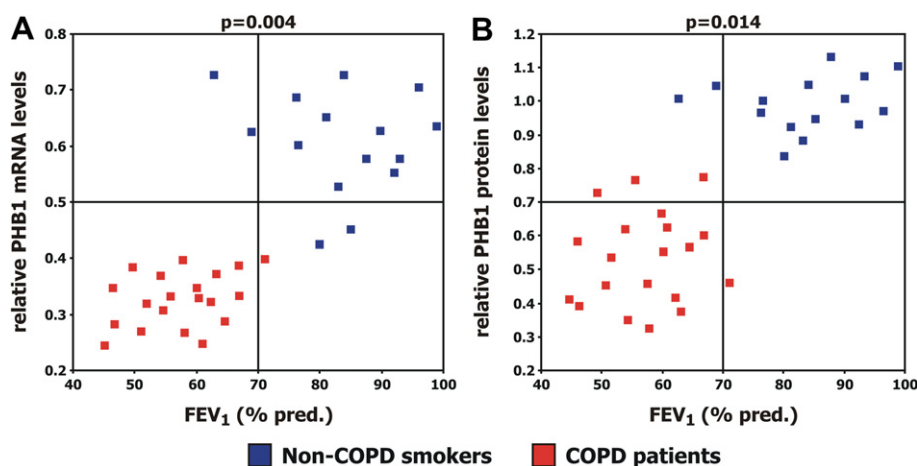


Figure 4 PHB1 mRNA (A) and protein expression (B) in relation to FEV₁ in non-COPD smokers (blue) and COPD patients (red). (For interpretation of the references to colour in this figure legend, the reader is referred to the web version of this article.)

Conflict of interest statement

None declared.

References

- Yoshida T, Tuder RM. Pathobiology of cigarette smoke-induced chronic obstructive pulmonary disease. *Physiol Rev* 2007;**87**: 1047–82.
- Cosio MG, Saetta M, Agusti A. Immunologic aspects of chronic obstructive pulmonary disease. *N Engl J Med* 2009;**360**: 2445–54.
- Tzortzaki EG, Siafakas NM. A hypothesis for the initiation of COPD. *Eur Respir J* 2009;**34**:310–5.
- Noguera A, Batle S, Miralles C, Iglesias J, Busquets X, MacNee W, et al. Enhanced neutrophil response in chronic obstructive pulmonary disease. *Thorax* 2001;**56**:432–7.
- Rahman I, Biswas SK, Kode A. Oxidant and antioxidant balance in the airways and airway diseases. *Eur J Pharmacol* 2006;**533**: 222–39.
- Bowler RP, Crapo JD. Oxidative stress in airways: is there a role for extracellular superoxide dismutase? *Am J Respir Crit Care Med* 2002;**166**:S38–43.
- Kinnula VL, Crapo JD. Superoxide dismutases in the lung and human lung diseases. *Am J Respir Crit Care Med* 2003;**167**: 1600–19.
- Camougrand N, Rigoulet M. Aging and oxidative stress: studies of some genes involved both in aging and in response to oxidative stress. *Respir Physiol* 2001;**128**:393–401.
- Mishra S, Murphy LC, Murphy LJ. The prohibitins: emerging roles in diverse functions. *J Cell Mol Med* 2006;**10**:353–63.
- Merkwirth C, Langer T. Prohibitin function within mitochondria: essential roles for cell proliferation and cristae morphogenesis. *Biochim Biophys Acta* 2009;**1793**:27–32.
- Artal-Sanz M, Tavernarakis N. Prohibitin and mitochondrial biology. *Trends Endocrinol Metab* 2009;**20**:394–401.
- Artal-Sanz M, Tavernarakis N. Prohibitin couples diapause signalling to mitochondrial metabolism during ageing in *C. elegans*. *Nature* 2009;**461**:793–7.
- Theiss AL, Sitaraman SV. The role and therapeutic potential of prohibitin in disease. *Biochim Biophys Acta* 2011;**1813**: 1137–43.
- Kasashima K, Ohta E, Kagawa Y, Endo H. Mitochondrial functions and estrogen receptor-dependent nuclear translocation of pleiotropic human prohibitin 2. *J Biol Chem* 2006;**281**: 36401–10.
- Kuramori C, Azuma M, Kume K, Kaneko Y, Inoue A, Yamaguchi Y, et al. Capsaicin binds to prohibitin 2 and displaces it from the mitochondria to the nucleus. *Biochem Biophys Res Commun* 2009;**379**:519–25.
- Ikonen E, Fiedler K, Parton RG, Simons K. Prohibitin, an anti-proliferative protein, is localized to mitochondria. *FEBS Lett* 1995;**358**:273–7.
- Tatsuta T, Model K, Langer T. Formation of membrane-bound ring complexes by prohibitins in mitochondria. *Mol Biol Cell* 2005;**16**:248–59.
- Kasashima K, Sumitani M, Satoh M, Endo H. Human prohibitin 1 maintains the organization and stability of the mitochondrial nucleoids. *Exp Cell Res* 2008;**314**:988–96.
- Ross JA, Nagy ZS, Kirken RA. The PHB1/2 phosphocomplex is required for mitochondrial homeostasis and survival of human T cells. *J Biol Chem* 2008;**283**:4699–713.
- Schleicher M, Shepherd BR, Suarez Y, Fernandez-Hernando C, Yu J, Pan Y, et al. Prohibitin-1 maintains the angiogenic capacity of endothelial cells by regulating mitochondrial function and senescence. *J Cell Biol* 2008;**180**:101–12.
- Bourges I, Ramus C, Mousson de Camaret B, Beugnot R, Remacle C, Cardol P, et al. Structural organization of mitochondrial human complex I: role of the ND4 and ND5 mitochondria-encoded subunits and interaction with prohibitin. *Biochem J* 2004;**383**:491–9.
- Theiss AL, Idell RD, Srinivasan S, Klapproth JM, Jones DP, Merlin D, et al. Prohibitin protects against oxidative stress in intestinal epithelial cells. *FASEB J* 2007;**21**:197–206.
- Henschke P, Vorum H, Honore B, Rice GE. Protein profiling the effects of in vitro hyperoxic exposure on fetal rabbit lung. *Proteomics* 2006;**6**:1957–62.
- Pauwels RA, Buist AS, Calverley PM, Jenkins CR, Hurd SS. Global strategy for the diagnosis, management, and prevention of chronic obstructive pulmonary disease. NHLBI/WHO global initiative for chronic obstructive lung disease (GOLD) workshop summary. *Am J Respir Crit Care Med* 2001;**163**:1256–76.
- Zmijewski JW, Lorne E, Zhao X, Tsuruta Y, Sha Y, Liu G, et al. Mitochondrial respiratory complex I regulates neutrophil activation and severity of lung injury. *Am J Respir Crit Care Med* 2008;**178**:168–79.
- Merkwirth C, Dargazanli S, Tatsuta T, Geimer S, Lower B, Wunderlich FT, et al. Prohibitins control cell proliferation and apoptosis by regulating OPA1-dependent cristae morphogenesis in mitochondria. *Genes Dev* 2008;**22**:476–88.

27. Janssens JP, Pache JC, Nicod LP. Physiological changes in respiratory function associated with ageing. *Eur Respir J* 1999; **13**:197–205.
28. Siganaki M, Koutsopoulos AV, Neofytou E, Vlachaki E, Psarrou M, Soultzis N, et al. Deregulation of apoptosis mediators' p53 and bcl2 in lung tissue of COPD patients. *Respir Res* 2010; **11**:46.
29. Vlachaki EM, Koutsopoulos AV, Tzanakis N, Neofytou E, Siganaki M, Drositis I, et al. Altered surfactant protein-A expression in type II pneumocytes in COPD. *Chest* 2010; **137**:37–45.